

Received June 17, 2020, accepted July 23, 2020, date of publication July 27, 2020, date of current version August 6, 2020.

Digital Object Identifier 10.1109/ACCESS.2020.3012195

A Fuse Saving Scheme for DC Microgrids With High Penetration of Renewable Energy Resources

NAVID BAYATI¹, HAMID REZA BAGHAE², (Member, IEEE), AMIN HAJIZADEH¹, (Senior Member, IEEE), AND MOHSEN SOLTANI¹, (Senior Member, IEEE)

¹Department of Energy Technology, Aalborg University Esbjerg, 6700 Esbjerg, Denmark

²Department of Electrical Engineering, Amirkabir University of Technology, Tehran 15875-4413, Iran

Corresponding author: Navid Bayati (nab@et.aau.dk)

ABSTRACT The high penetration of renewable energy resources (RERs) increases the fault current level of direct current (DC) microgrids and causes bidirectional flow for fault current. Therefore, it may cause a miscoordination between fuses or other protection devices. The traditional coordination methods are based on shifting the operation curve of protection devices below the characteristic curve of the fuses during temporary faults to save fuses. However, in case of low variations of the system topology and low impedance faults, these methods can be used to save fuses. Also, in the case of high penetration of RERs, due to the variations of the short circuit level, the traditional methods are not effective. On the other hand, due to the lack of standards and proper protection methods in the DC microgrids, presenting a recloser switch – fuse coordination scheme for DC microgrids is essential. To address these issues, this paper proposes a fuse saving method by finding the appropriate setting of fuses and the recloser switch, which is effective for DC microgrids with various types and penetration levels of RERs. The proposed protection method is localized, and without communication links, it is applicable for both digital and conventional protection devices installed in the DC microgrids. The proposed scheme formulates the fuse-recloser switch coordination challenge as a curve-fitting problem and solves this problem to obtain the settings of the digital recloser switch and fuse. The proposed strategy provides a robust setting for fuse and digital recloser switch by considering different topologies of the DC microgrids. The proposed method is applied to a DC microgrid in different scenarios. The effectiveness and robustness of the proposed method are illustrated by digital time-domain simulation studies in the MATLAB/Simulink software environment and comparisons with previously-reported protection strategies.

INDEX TERMS DC microgrid, fuse, protection, recloser switch, renewable energy resources.

I. INTRODUCTION

In recent years, DC microgrids have been used widely as a realistic scheme with the majority of DC loads and sources such as storage devices, fuel cells, and photovoltaic (PV) units [1] and [2]. DC microgrids reduce the number of converters compared to the alternating current (AC) systems, and it reduces the power losses [3]. In DC microgrids, one of the main challenges is the lack of effective protection strategy and standard [4]. Protecting the DC Microgrid against fault is difficult due to the variation of topology, lack of zero-crossing point, and presence of the power converters [5].

In DC microgrids, the components are protected by using fuses and recloser switches [6]. Fuses are typically placed as

series with the components and at a remote position from the grid side. During a temporary fault at any part of the system, the corresponding fuses should not melt, and the fast operation performance of the recloser switch removes the path of fault feeding from the grid side. It allows the temporary fault to clear itself [7]. Also, during the permanent faults, the fuse must clear the fault by melting before the trip operation of the recloser switch to prevent interruption of loads between the recloser switch and fuse. In other words, during the temporary faults, the fuse is the backup protection device, while during the permanent faults recloser switch is the backup protection device. Weak coordination between the protection devices causes transient voltage interruption and voltage sag [8] and [9] that specify the overall power quality of the system. Thus, proper coordination between the fuses and recloser switch is essential. The coordination of fuse

The associate editor coordinating the review of this manuscript and approving it for publication was Jenny Mahoney.

and recloser are discussed in [10] for distribution systems of power systems without the presence of RERs.

Moreover, in the radial DC microgrids, the fault current is unidirectional; however, by installing RERs in different locations, the fault current will be bidirectional. Besides, installing an additional RERs in DC Microgrid changes the short circuit level of every node of the system. Therefore, the probability of the miscoordination in the fuse and recloser switch operation increases.

Protection coordination of fuses and recloser switch during the high penetration of RERs is a challenging task. In recent years, the coordination problem of these protection devices has been well studied for AC systems. In [11], the distribution system has been divided into different zones to propose an adaptive protection coordination strategy for fuse and recloser in the presence of RERs. Further, an adaptive setting for recloser has been proposed in [12] to coordinate the fuse and recloser by modifying the instantaneous overcurrent and time delay elements of the recloser. In these methods, implementing a communication channel is essential, and they require a remote control for the system. The maximum RER injection during the fault without affecting the fuse and recloser coordination in a radial distribution system have been discussed in [13]. Also, in [14], the RER locations, fuse, and recloser characteristic curves have been modified to maintain the coordination of fuse-recloser. This method improves coordination by decreasing the number of fuse-recloser miscoordination cases. Also, the impact of inverter-based resources on the miscoordination of fuse-recloser has been investigated in [15]. Also, the fuse and recloser coordination have been adjusted by using the directional properties of the microprocessor-based reclosers. The mentioned methods have been developed for implementing in the AC systems, while the usage of DC systems is widely increased in recent years.

On the other hand, due to the difference in the nature of DC and AC, to correctly selecting of a DC fuse for DC microgrids, the capabilities of fuse and critical parameters of the system should be known. In some applications, the AC fuses can be used in DC systems. However, there are no specific roles that safely convert an AC voltage rating to DC voltage rating [16]. In AC systems, on the frequency of 60 Hz, the current crossing at zero point 120 times per second. But, due to the lack of a zero-crossing point in DC systems, DC fuse should be able to absorb and extinguish the total energy of the DC arc. Therefore, the DC fuses should be designed especially for use in the DC systems. In [17], the analysis of an active fuse in DC fault is carried out. The active fuses consist of two components, a passive cutout bridge, and an active switch. During the fault, the active switch is activated by a signal, and when the switch is released, an excess fault current flows via the cutout bridge and melts it, and finally, the current path is interrupted. In [18], a model for calculating the melting time of a DC fuse is proposed to model voltage fluctuations and fault current from start point to melting point.

One of the other main components of protection schemes in DC Microgrids is the recloser switch. Similar to AC systems, the system recovery of DC Microgrids can be realized by the reclosing operation of protection devices. However, due to the different working principles, the operation time of AC breakers are in the range of 40-60 ms, while DC breakers can operate within 3 ms. Also, DC systems have no zero-crossing point. Thus, reclosing operation in the DC Microgrids should be considered. The application of the recloser switches in the DC distribution networks has been discussed in [19] to protect the system against temporary faults considering the high inrush current and avoiding the false tripping. In [20], a DC breaker reclosing operation is suggested, and a novel sequential auto reclosing strategy for DC grids is presented. Therefore, the potential adverse impacts such as damage to power electronic devices and line insulation failure due to the using traditional reclosing schemes are eliminated. Also, a recloser switch for DC distributed systems is suggested in [21], which uses DC thyristors to provide low conduction losses and quick recloser switch.

However, the installation of fuses and recloser switches in a DC system without considering the coordination between these protection devices deteriorates the overall operation of the protection system. The coordination between the DC circuit breaker and fuses for maritime DC Microgrid has been discussed in [22]. In this method, the settings of the DC circuit breakers have been adjusted first, and then the proper fuse has been selected to be used in the system. This method causes difficulty in the selection of fuses due to the lack of availability of a wide range of characteristics of fuses. Also, to reduce cost and shutdown time, the main aim of the fuse-recloser switches should be saving fuses, which has a lack of enough research.

In the studies mentioned above, the time dial setting (TDS) of the recloser for both slow and fast modes has been selected for coordinating with the time-current characteristics of the fuse. Further, because the majority of the mentioned studies have been focused on the AC systems, further studies should be done to address the fuse-recloser switch coordination problem in the DC microgrids. Also, due to the variation of the RERs power injection and high penetration of RERs in these systems, a special coordination method for DC microgrids is essential.

This paper presents a local fuse saving method by proper coordination between fuse and recloser switch in DC microgrids. The main contribution of this paper is a new non-standard switch characteristic for fast tripping of recloser switches to avoid miscoordination with fuses in DC Microgrids. The proposed strategy uses a series of constraints to provide a robust coordination scheme for different operation modes and situations. The characteristic curve of the recloser switch is modified by a coefficient to improve the speed and coordination of fuse and recloser switch. Moreover, to maintain the coordination of these protection devices, the constraints of the proposed method ensure robust operation of recloser by providing an approximately constant distance

between both characteristic curves. Finally, to evaluate the performance of the proposed algorithm, offline digital time-domain simulation studies are carried out on a test micro-grid system in MATLAB/Simulink software environment, and also the results are compared with previously reported methods.

The remainder of the paper is organized as follows: Section II discusses the behavior of the fuses and reclosers in the DC system. Section III discusses the proposed fuse saving and coordination scheme. The performance of the proposed coordination method is validated by simulation results in section IV for different scenarios. Finally, section V concludes this study.

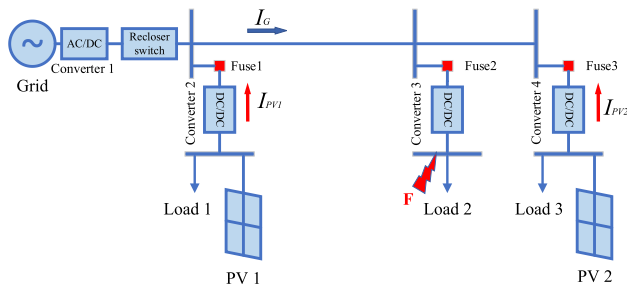


FIGURE 1. The structure of a radial DC microgrid.

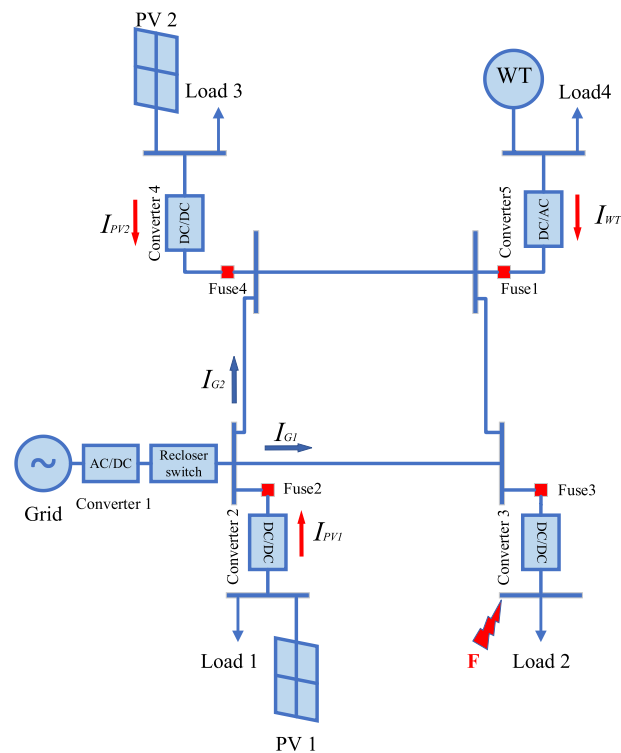


FIGURE 2. The structure of a ring DC microgrid.

II. FAULT CALCULATIONS OF DC FUSES AND REclosERS

In this section, the performance of DC fuses and reclosers during the fault in DC Microgrids are investigated. There are two types of DC microgrids in terms of the structure of

the system; ring and radial systems. In the radial systems, all loads are fed by the grid by a unidirectional power flow. However, due to the existence of the RERs, loads are fed by RERs by a bidirectional power flow. As shown in Fig. 1, the fault current is made by three different current sources, I_G by grid through an AC/DC converter, and I_{PV1} , and I_{PV2} injected by PV₁ and PV₂, respectively. The structure of a ring DC Microgrid is shown in Fig. 2. Despite the unidirectional flow of the grid current in radial systems, the fault is fed by grid in-ring DC microgrids by a bidirectional current. Therefore, the value of fault current from the grid affects all lines of systems; thus, using a recloser switch on the place of converter₁, as shown in Fig. 2, can control the fault current during the temporary faults to save the fuses. Also, all RERs in the system contribute to supplying the fault current from both sides of the fault. Therefore, it increases the complexity of coordinating the fuse and recloser switch.

During fault in DC systems, the behavior of the system can be categorized into three stages, 1) capacitor-discharge, 2) conducting freewheeling diode, 3) current from the converter. Immediately after occurring the fault, the capacitors of converters start to inject high rise current to the faulty point. And after 1 or 2 ms, capacitors are completely discharged, and the second stage will start. At the second stage, the equivalent circuit of the system will be an inductance-resistance circuit. Therefore, due to the high melting time of DC fuses, compared to recloser switches, the operation curve of recloser switches and DC fuses can be defined during the first and second stages, respectively.

In selecting a DC fuse, the challenging part is finding the operation time of DC fuse based on the fault characteristic. In determining the operation time, because the fault current rise is based on the L/R , a time constant, the inductances of system and arc have significant differences. In AC systems, by using the AC fuses, the melting times can be from 4 ms to a few cycles. However, in DC systems, because the fault current requires more time to reach the steady-state value, the DC fuse takes more time to sense the fault current. For example, in a DC Microgrid with an L/R lower than 10 ms, the DC fuse curve is the same as the operation curve of AC fuses, but at the higher current portion of the curve, it has a minor difference. For an L/R higher than 10 ms, there is a slowing isolating of the fault by fuses, due to a slow increase in fault current. The effect of L/R on the operation of DC fuses and comparing with an AC fuse is shown in Fig. 3. Based on this figure, only DC fuses for a component with low value of L/R can use the characteristic curve of AC fuses. For instance, in most cases, the L/R value of batteries is approximately 2 ms.

Based on the difference between DC and AC fuses, the characteristic curve of a DC fuse should be defined in terms of L/R . During a fault in a DC system, the DC line can be equivalented by the inductance-resistance circuit. Therefore, the fault current can be defined by [23]:

$$I_i = I_f(1 - e^{-n}) \quad (1)$$

TABLE 1. Converting AC fuse curve to DC fuse curve.

I_{fuse}	t_{fuse}	L/R	n	I_{DCfuse}	L/R	n	I_{DCfuse}
29999.2	0.015793	0.005	3.1586	40387.75	0.01	1.5793	54973.87
2217.04	0.032707	0.005	6.5414	2524.69	0.01	3.2707	2951.10
160.763	0.071207	0.005	14.2414	169.96	0.01	7.1207	180.921
59.26	0.115076	0.005	23.0152	61.29	0.01	11.507	63.546
24.6046	0.263379	0.005	52.6758	24.96	0.01	26.337	25.33
12.7934	0.789654	0.005	157.930	12.85	0.01	78.965	12.91
8.71405	2.64545	0.005	529.09	8.72	0.01	264.54	8.738
7.37383	10.266	0.005	2053.2	7.37	0.01	1026.6	7.379
7.24229	14.7588	0.005	951.76	7.24	0.01	1475.88	7.245

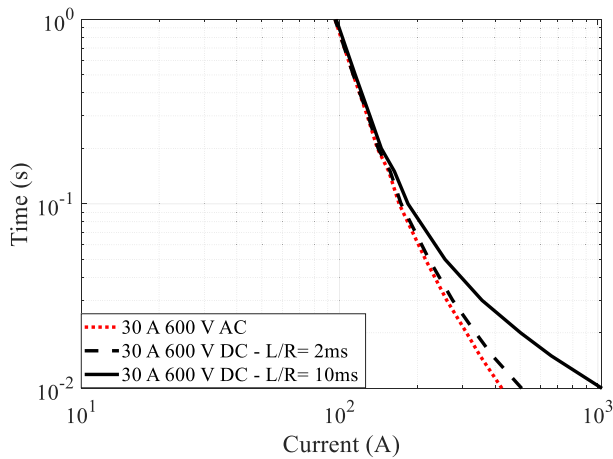


FIGURE 3. Effect of L/R on fuse curves.

where I_i is the instantaneous current, n is the number of the time constant, and I_f is fault current, and it is determined by the initial value of voltage, V , and resistance, then I_f is V/R . On the other hand, the heating effect of DC fuses during melting is calculated by the RMS value of (1) as follows:

$$I_{rms} = \left(\frac{1}{T} \int_0^T i^2(t) dt \right)^{0.5} \quad (2)$$

where T is the period over which integrated or the number of time constants. By substituting of (1) into (2), the I_{rms} is obtained by:

$$I_{rms} = I_f \left(1 + 2 \frac{e^{-n}}{n} - \frac{e^{-2n}}{2n} - \frac{1.5}{n} \right)^{0.5} \quad (3)$$

Moreover, the value of n is tR/L . On the other hand, the characteristic curve of AC fuses obtained by [14]:

$$\log(t_{fuse}) = a \log(I_{fuse}) + b \quad (4)$$

where a and b are the settings of fuse, I_{fuse} is the fault current through AC fuse, and t_{fuse} is the operation time of fuse. Based on (3), the characteristic curve of DC fuses can be presented by

$$\log(t_{fuse}) = a \log \left(\frac{I_{DCfuse}}{\left(1 + 2L \frac{e^{-tR/L}}{tR} - L \frac{e^{-2tR/L}}{2tR} - L \frac{1.5}{tR} \right)^{0.5}} \right) + b \quad (5)$$

where I_{DCfuse} is the fault current through DC fuse. Therefore, (5) can be used as the characteristic curve of DC fuses. Also, it could be noted that the value of n is replaced with tR/L to define a time-based equation (5). For example, in Table 1, a time-current curve of an AC fuse, SMU-40, is converted to the DC fuse curve by using (5) for two different time constant values. It indicates that the higher value of time-constant causes more differences in values of I_{DCfuse} with I_{fuse} , especially in lower time. The algorithm for converting the time-current characteristic curve is summarized as follows:

1. Find the points of the time-current curve of fuse and determine the related times and currents.
2. Define the number of time constants.
3. Solve (3).
4. Plot (3) in terms of the time of plots.
5. Select another point at the time-current curve and repeat steps 1 to 4.

Different types of protection devices such as recloser switches, fuses, solid-state circuit breakers, and relays are used in the DC microgrids. The main aim of an effective protection system is clearing both permanent and temporary faults as quickly as possible and de-energizing the minimum zones of the DC Microgrid. In DC microgrids, faults are often temporary and caused by transient contacting of an energized line. The temporary faults are cleared themselves after flowing the current through the fault path. On the other hand, the fast operation of the recloser switch and fuses should be coordinated to avoid the unnecessary melting of fuses, and consequently, it saves the fuses.

Also, the current based relays with the characteristic curve of Fig. 4 are implemented in DC Microgrids [24]. And, the fast operation curve of these relays is adjusted to be under the fuse curve. However, due to the increasing the maximum of fault current by installing a RERs or changing topology, from $I_{F,max}$ to I_1 , the coordination between relay and fuse will eliminate. Also, due to the slow operation of these relays, the traditional relays cannot be implemented in the DC microgrids protected by fuses. Consequently, downstream fuses should be coordinated by the operation of a recloser switch. Therefore, the operation curve of the recloser switch for permanent fault should be located in the upper area of the fuse curve, and the temporary fault should be in the lower area of the fuse curve.

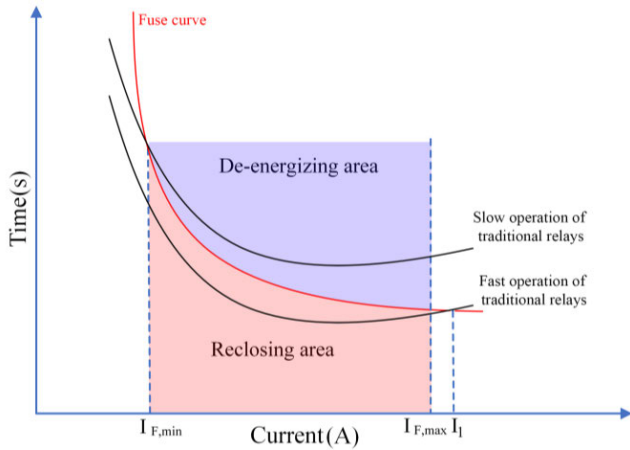


FIGURE 4. The characteristic curve of fuse.

Evaluating the selectivity of fuses between downstream and upstream fuses is common in the microgrid research today. Time current curve is compared to determine the selectivity of events, and fuses are presumed to be selective if a separation between the total clearing curve of the downstream fuses and the minimum melting curve of the upstream fuses is maintained. It should be noted that fuse clearing and melting I^2t values should be compared for assessing the selectivity of fuses. The I^2t value of downstream DC fuses should be less than the melting I^2t value of upstream DC fuses for selectivity during faults. In this paper, because the backup of the downstream DC fuses is recloser switch, therefore, by appropriate coordination between DC fuses and recloser switch, the selectivity of the protection system will be ensured.

III. PROPOSED PROTECTION STRATEGY AND COORDINATION FOR RECLOSER SWITCH AND FUSE

When a fault occurs in a DC Microgrid, the IGBT switches of converters are blocked and leaves the antiparallel diodes exposed to the fault current. This means that during the fault, and collapsing voltage, the current flows through diodes, and cannot be limited. However, typically, the fault current tolerant of diodes is high, but the thermal limit of diodes, which determines by I^2t should be considered during the selection of fuses. For example, the maximum non-repetitive surge current of diode NTE5338 is 1500 A, and the maximum I^2t is 9350 A²sec. Then, the capacitors of converters start to discharge through the lines. The equivalent circuit of a DC line is shown in Fig. 5. The fault current of this circuit from the AC side can be calculated by [25]

$$\begin{cases} I_{Fseen}(t) = \frac{V_0}{L_1\omega} e^{-\alpha t} \sin(\omega t) \\ \quad + I_0 e^{-\alpha t} (\cos(\omega t) - \frac{\alpha}{\omega} \sin(\omega t)) \\ \alpha = \frac{R_1 + R_F}{2L_1} \\ \omega = \sqrt{\frac{1}{L_1 C_1} - \alpha^2} \end{cases} \quad (6)$$

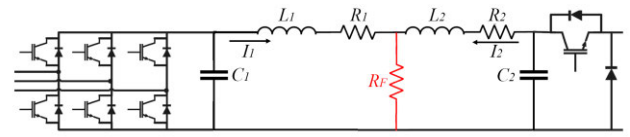


FIGURE 5. Equivalent circuit of a DC line, connected to AC grid and DC/DC converter during fault.

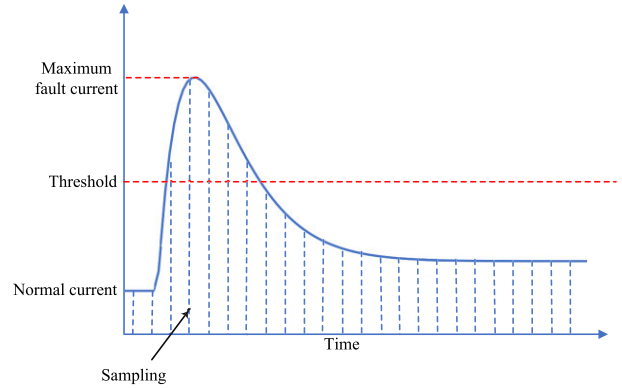


FIGURE 6. Fault current behavior during fault.

where I_{Fseen} is the fault current that seen by the recloser switch, V_0 and I_0 are initial voltage and current, respectively. R_1 and L_1 are the resistance and inductance from AC/DC converter to the fault location. C_1 is the capacitor of the AC/DC converter, and R_F is the fault resistance. During the capacitor discharge stage, the fault current is shown in Fig. 6. By Differentiating (6), the maximum value of fault current occurs at

$$t_{max} = \frac{1}{\omega} \tan^{-1} \left(\frac{2\alpha\omega I_0 - \omega V_0/L}{\alpha^2 I_0 - I_0\omega^2 - \alpha V_0/L} \right) \quad (7)$$

where t_{max} is the time of the maximum value of the current. Also, the value of fault current cannot exceed the short term thermal tolerant of components. Therefore, a new current factor for the setting of recloser switches is defined by

$$I_{Setting} = \sigma - I_{F,max} \quad (8)$$

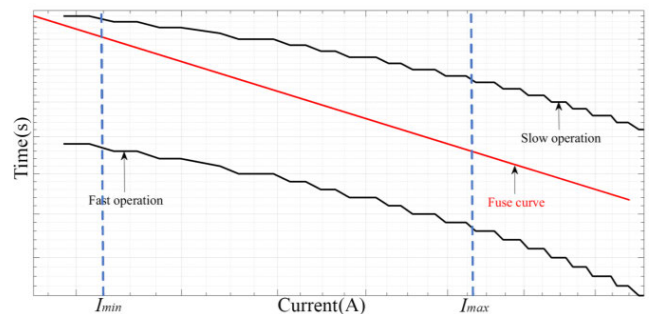


FIGURE 7. The inverse time-current characteristic curve of the proposed recloser switch.

where, $I_{Setting}$ is the current setting of recloser switch, and σ is the short term thermal tolerant of the conductor. Therefore, (7) and (8) are used for setting the recloser switch of AC/DC converter. For this aim, the recloser switch uses the $I_{Setting}$

and t_{max} for the setting of the switch, and the $I-t$ curve of the recloser switch is an inverse time-current curve, as shown in Fig. 7. The fast operation curve of the recloser switch is responsible for temporary faults and should be located below the fuse characteristic curve. Moreover, the slow operation curve of the switch for permanent faults is located above the fast operation curve with a time delay. The proposed $I-t$ curve is depicted in Fig. 7. Moreover, to determine a general equation for the characteristic curve of recloser switch, the data of the maximum fault current and the corresponding time are estimated by two exponential terms, as indicates in (9):

$$t_{max} = Ae^{-BI_{settings}} + Ce^{-DI_{settings}} \quad (9)$$

where A , B , C , and D are the constant settings of the recloser switch. Moreover, due to the exponential nature of the fuse and recloser switch curve, these curves will be depicted in logarithmic figures. Therefore, the fuse characteristic curve should be located between these two curves. After the fault detection, based on the fault current, the recloser switch cut the power line, then after a specific delay, if the fault is cleared, the system will back to the normal operation; however, if the fault is still in the system, recloser switch trips again. Based on the standards of AC protection systems, three times, a recloser should check the fault. Then, if the fault is still in the system, the fuse will be de-energized the faulty section. The slow operation curve is the backup of the fuse. The flowchart of the proposed method is depicted in Fig. 8. Therefore, by considering the characteristic of DC microgrids, high rise current, and low tolerant of DC components to high fault current, the proposed scheme clear both temporary and permanent faults by lowest operation time.

In this method, two delays should be identified for setting the slow operation time of the switch, and coordination between fast operation time of recloser switch with the fuse. All conductors of DC Microgrid have a thermal limit, which shows by I^2t curve. Therefore, the slow operation of the recloser switch should be in the below part of the thermal limit curve. Thus, the fuse characteristic curve should be between these two curves. Therefore, the delay between the slow and fast operation curve is identified by τ . The values of a , and b of (5) should be calculated by curve fitting.

IV. SIMULATION RESULTS

To validate the effectiveness of the proposed method, the simulations are investigated on a DC Microgrid, as shown in Fig. 9. The case studied DC Microgrid is suggested for implementing in Rø mø island in Denmark consists of PV, fuel cell (FC), battery, and offshore wind turbine (WT), and several loads, and this system is connected to the grid by an AC/DC converter. Due to the low distance of Rø mø Island from the mainland, the suggested DC Microgrid can be operated both in islanded and grid-connected mode. To improve the use of RESs and the quality of living of residents, the PV-WT-FC-Battery is suggested for this island. The total electricity loads of this DC Microgrid in Rø mø Island are estimated to 696 kW. The system is composed of PV systems (400 kW

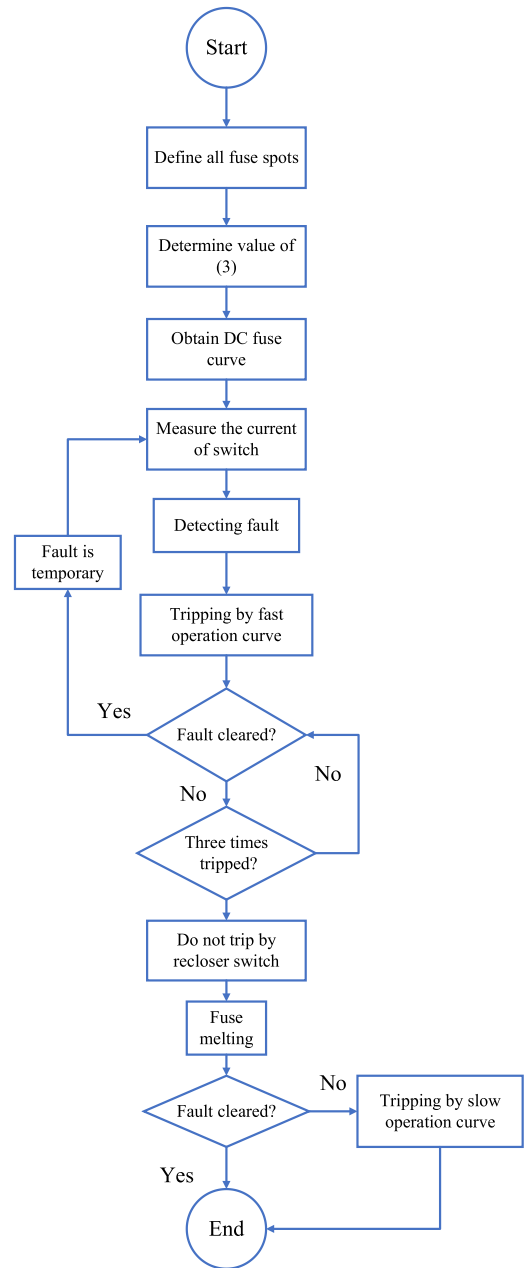


FIGURE 8. Flowchart of the proposed method.

in total), offshore WTs (300 kW), and an FC (15 kW). Also, Table 2 represents the detailed parameters of the test system. The protection scheme of the island is consist of component fuses, recloser switch, and overcurrent based relays for lines. The DC fuses are responsible for protecting other sections of DC Microgrid during faults in each component, and the recloser switch is responsible for protecting the system and saving DC fuses against temporary faults. Because the aim of this paper is saving fuses during temporary faults, the backup of fuses are a recloser switch. At the connection line between the grid and DC Microgrid, a recloser switch is installed. Moreover, the laterals are protected by fuses 1 to 8.

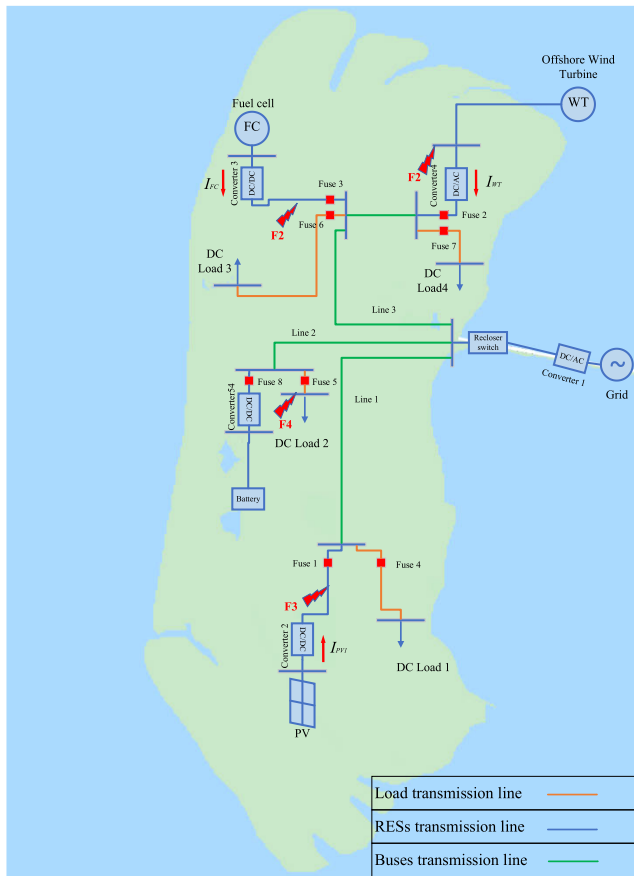


FIGURE 9. The under-study DC microgrid.

TABLE 2. Parameters of DC microgrid.

Component	Rate
PV	VOC=64.2 V, ISC= 5.96 A, 25 series module, 66 parallel strings, Series and parallel resistances for 1 module: 0.037 Ω and 993 Ω, respectively.
WT	700 kW, Reactance: 3.23 Ω
FC	100 kW, Ohmic loss per cell: 0.000328 Ω, number of cells: 1000
Battery	200 Ah, 0.1 Ω
Inductance of line	0.22 Ω
Resistance of line	0.2 Ω/km
Line lengths	Line ₁ : 3.5 km , Line ₂ :2 km , Line ₃ :3 km
Bus Impedances	0.1 Ω
Nominal voltage	500 V
Grid voltage	11 kV
Loads power	Load ₁ = 208 kW, Load ₂ = 113 kW, Load ₃ = 167 kW, Load ₄ = 208 kW

At the first stage, the values and times of maximum fault current for different locations and fault resistance are determined to find the curve for the fast operation curve of the recloser switch. The maximum value of load current is used for determining the range of detectable fault resistance. In other words, after increasing the 20% in the current, the fault is detected. Therefore, the maximum value of fault resistance should be responsible for causing a fault current equal to 20% overload. In this system, the range of fault resistance is between 0 to 16.6 Ω. In this system, by considering

the conductor thermal limits, the value of delay between slow and fast operation time of the recloser switch is set to $\tau = 0.9$.

The short circuit faults and coordination between recloser switch and fuses are studied using the MATLAB/Simulink software environment. Fuses installed in the laterals are divided into two groups, load and RESs fuses. The fuses number 4 to 7 are the load fuses, and other fuses are RESs fuses. In the fuses operation curve, the value of a is a negative parameter, and b is a positive value that is considered between 0 to 6.

TABLE 3. Fault current characteristics for fault in different laterals.

Fault resistance (Ω)	Fault lateral	Fault location (km)	Fault point	I_{Fmax} (A)	$I_{Recloser}$ (A)	t_{max} (ms)
0.2	Fuse ₈	2	F ₁	747	689	61.8
0.2	Fuse ₂	3	F ₂	425	368	84.6
0.2	Fuse ₄	3.5	F ₃	1608	1310	40.9
0.2	Fuse ₅	2	F ₄	736	714	79.3
0.6	Fuse ₈	2	F ₁	281	252	84.2
0.6	Fuse ₂	3	F ₂	216	193	84.5
0.6	Fuse ₄	3.5	F ₃	571	532	39.8
0.6	Fuse ₅	2	F ₄	280	254	90.1

To offline calculate the settings of the recloser switch, the arc faults are simulated at all fuse locations with different fault resistances. By using the data of the fault current magnitude and maximum time for all situations, the operation curve of the recloser switch is determined by (7) and (8). Thus, to cover all situations, the worst case of the fault current should be taken into account, and the fast operation curve should be in the lowest place in the $I-t$ curve. Table 3 shows the I_{Fmax} and t_{max} of several fault scenarios at the fuse laterals. Moreover, the fault distance from recloser bus is determined in Table 3, and the faulty points are indicated in Fig. 9. In the presented DC Microgrid, due to the low dependency to generator-based power resources, lower nominal voltage, and also considering the fault resistance in fault cases, compared to other DC grids, for example, HVDCs, the values of fault current are placed in a medium range of fault current.

It should be noted that in the fault at fuse 8 and 2 by fault resistance 0.2 Ω, the fault current from the main grid is 747 A and 425 A for the arc fault at the battery and WT buses, respectively. However, when the fault resistance grows to 0.6 Ω, the main grid current is decreased to 281 A and 216 A at the battery and WT laterals, respectively. If the fault resistance decreases, the fault current increases, and consequently, the operation time of the recloser switch should increase.

In the next step, the performance of the recloser switch is identified, and the parameters of the recloser setting are determined. For this aim, the values of the recloser setting are depicted as Fig. 10, and the parameters of estimation are shown. The depicted curve shows that by increasing the fault current, the operation time of the recloser switch decreases. The setting of recloser switch is defined by (9), and therefore an exponential curve fitting is performed by using data of Fig. 10 to find the values of A , B , C , and D . Therefore,

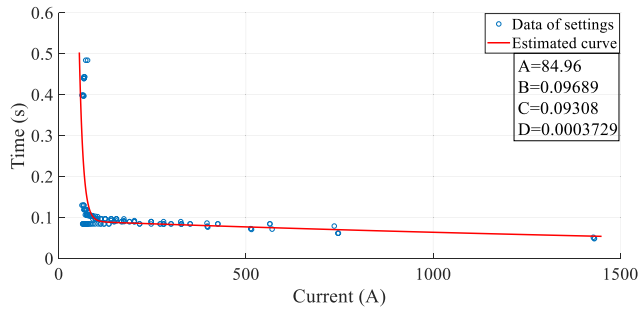


FIGURE 10. The estimation of the recloser switch setting.

the characteristic curve of recloser is defined by

$$t_{max} = 84.96e^{-0.09689I_{settings}} + 0.09308e^{-0.0003729I_{settings}} \quad (10)$$

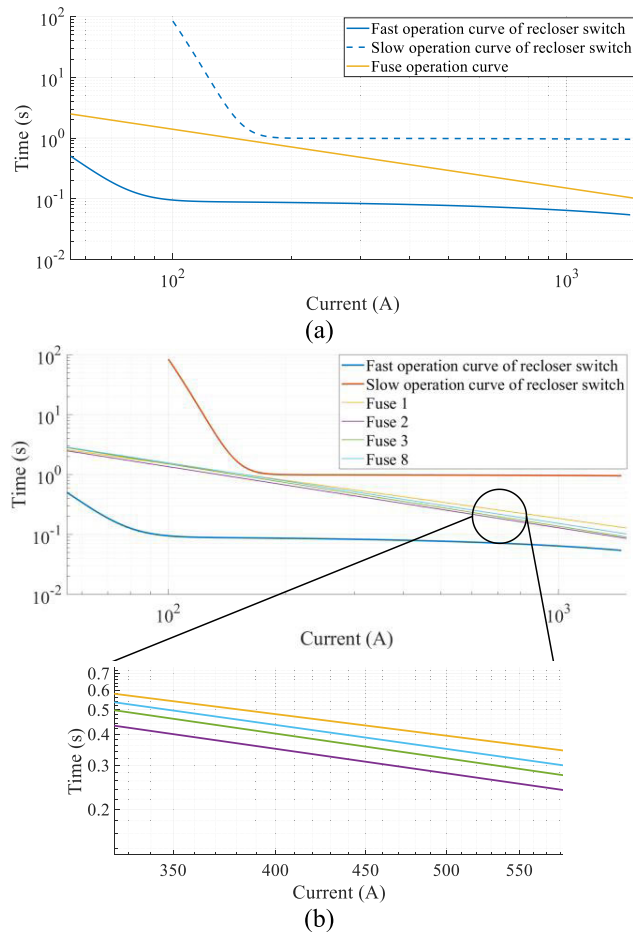


FIGURE 11. The operation curve of (a) load fuses (b) resource fuses.

It should be noted that the least-squares fitting-exponential calculates the curve fitting. Therefore, the $I-t$ curve of the recloser switch by adding τ to the fast operation curve is shown in Fig. 11. At the next stage, the fuse operation curves are determined by curve fitting, which should be adjusted based on the worst-case in fault current on the installed branch. The curve fitting is performed by using an optimization algorithm, the genetic algorithm in this paper, to find the best values of settings subjected to placing between recloser

switch curves. Therefore, the DC fuse curve of load fuses are defined by

$$\log(t_{fuse}) = -0.95 \log\left(\frac{I_{DCfuse}}{(1 + 2L \frac{e^{-iR/L}}{iR} - L \frac{e^{-2iR/L}}{2iR} - L \frac{1.5}{iR})^{0.5}} + 4.8\right) \quad (11)$$

Moreover, the value of L/R of loads in this paper is assumed to be 2 ms. The fuse operation curves of fuses 1 to 8 are depicted in Fig. 11, and the settings are represented in Table 4. In Fig. 11 (a), the time-current curve of Fuses number 4 to 7 are indicated. These fuses are load DC fuses; therefore, due to the same behavior of these loads, the characteristic curve of them are the same. Which is located between the slow and fast operation curve of the recloser switch. On the other hand, other resources DC fuses have a different time-current curve, as shown in Fig. 12 (b). In these curves, DC fuse2 has the lowest operation curve, and DC fuse1 has the highest one. The reason for this has a different fault current magnitudes. The difference between the settings of fuses is due to the difference between the maximum value of the fault current of the protected branch by the corresponding fuse. For the case of installing an additional RESs or increasing the value of fault current, the maximum value of fault current will increase, however, due to the approximately fixed margin between fuse and recloser switch curve, it cannot jeopardize the operation curve of recloser switches in higher fault currents.

TABLE 4. The settings of the fuses.

Fuse number	a	b
Fuse ₁	-0.89	4.6
Fuse ₂	-1.01	5.0
Fuse ₃	-1.01	5.2
Fuse ₄	-0.95	4.8
Fuse ₅	-0.95	4.8
Fuse ₆	-0.95	4.8
Fuse ₇	-0.95	4.8
Fuse ₈	-0.99	5.1

Also, during the fault, the fault current behavior in the recloser switch is shown in Fig. 12 (a) for a temporary fault at load 1 location with fault resistance of 1.5 Ω . During the fault, the fault current increases to 253 A, as shown in Fig. 12, and then after approximately 90 ms, it reaches the steady-state value of fault current. Based on Fig. 12 (a), the recloser switch is tripped in 84.3 ms, and after a delay of 16 ms, the recloser switch is closed, and the DC Microgrid is restored to the normal operation mode. On the other hand, for investigating the impact of source and line impedances, in Fig. 12 (b), these impedances are neglected. Therefore, the magnitude of fault current increased to 387 A. Then, the recloser switch will operate within a lower operation time than Fig. 12 (a) by 76.2 ms.

This operation of recloser does not permit the fuses to melt during the temporary faults. Furthermore, based on Fig. 13, the characteristic curves of recloser switch and load DC

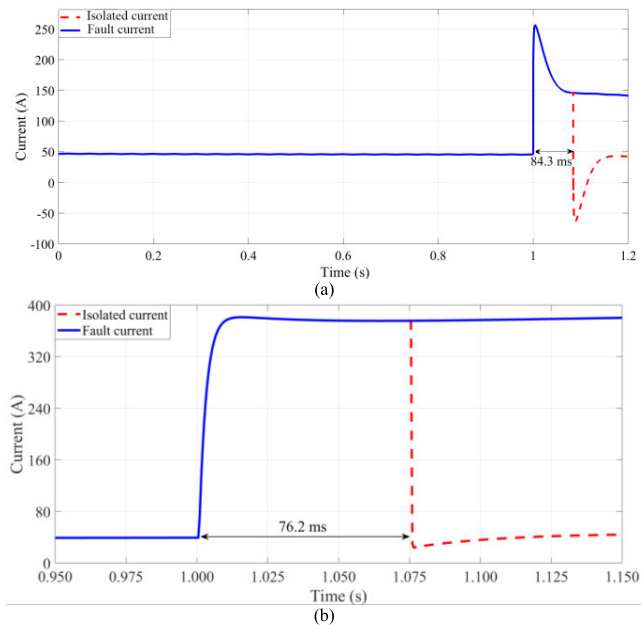


FIGURE 12. The fault current behavior with and without recloser switch (a) by considering the resistance of lines and sources (b) ignoring the resistances of lines and resources.

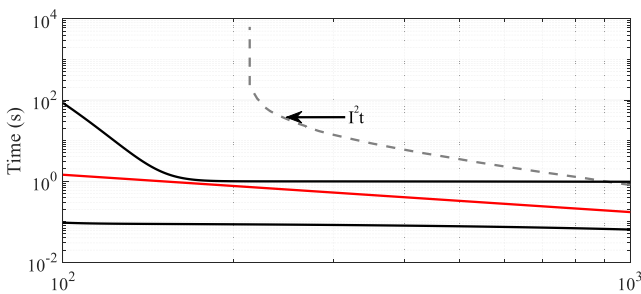


FIGURE 13. The fuse- recloser switch characteristic curve and the thermal limit curve.

fuse are designed based on I^2t curve of load 1. Therefore, the operation of recloser and fuse ensure the safety of load 1 during the fault.

For the investigation of the proposed method during faults, faults with different scenarios are applied to the test system, and the results are shown in Table 5. Based on Table 5, during the temporary faults, recloser trips in less than 130 ms, and 90 ms for fault current less than 100 A, and more than 100 A, respectively, to save fuses. It can be seen during the low fault resistances, the high fault current can be dangerous for all components of the DC microgrids, and therefore, by using the proposed method, the clearing time of low fault resistance faults is to lower than other types of faults, which it ensures the safety of all components of the system. Moreover, the impact of line outages on the performance of the proposed method is evaluated. During the line outages, for example, Line1 outages during a fault on the battery with fault resistance of 3 Ω , the recloser switch operates during 98 ms to save the fuses of downstream. The results of Table 5 show the robustness of the proposed method against variations of fault resistances, line, and power resource outages.

TABLE 5. The operation times of the recloser and fuses in different scenarios.

DC Microgrid scenario	Faulty branch	Operation time (ms)	
		Recloser switch	Fuse
Fault type=temporary, PV outages, Fault resistance=1.1 Ω	DC Load 2	84	--
Fault type=temporary, WT outages, Fault resistance=0.8 Ω	PV	61	--
Fault type=temporary, FC outages, Fault resistance=0.4 Ω	Battery	71	--
Fault type=temporary, Line1 outages, Fault resistance=3 Ω	Battery	98	--
Fault type=permanent, PV outages, Fault resistance=1.1 Ω	WT	--	394
Fault type=permanent WT outages, Fault resistance=0.8 Ω	FC	--	181
Fault type=permanent, FC outages, Fault resistance=0.4 Ω	DC Load 3	--	259
Fault type=permanent, Line 3 outages, Fault resistance=3 Ω	DC Load 2	--	412

In the first and fourth scenarios, all RERs produce at the full capacity, and the fault resistance is zero, which makes the worst situation for the fault current. Therefore, during the temporary fault, the recloser switch trips by the lowest operation time compared to other scenarios. Also, during the permanent fault, the fuse melts at the lowest time compared to other scenarios. In general, it can be shown that fuse saving is achieved in all scenarios under different fault conditions. In other words, the recloser switch operates before the fuses for temporary faults. The results show that the proposed method can save the fuses and clear the fault in different conditions by a scheme which is specially designed to implement in DC microgrids.

A. COMPARATIVE ASSESSMENTS

To compare the performance of the proposed protection strategy with the existing recloser-fuse coordination methods, it should be noted that there is a lack of study of recloser-fuse coordination on the DC Microgrids. Therefore, in this section, the qualitative and quantitative comparison between the proposed method and existing protection coordination approaches for other protection devices on the DC Microgrids are compared and shown in Table 6. It is observed from Table 6 that the proposed strategy coordinates the fuse and recloser switches irrespective of RESs output and fault location and resistance. Moreover, it is a costless scheme that can be implemented easily in practical systems. In the proposed method, the recloser switch is coordinated with lateral fuses by considering the variation of fault current. Also, this method is a local scheme that causes higher reliability and lowers cost due to the lack of communication channels. Therefore, in terms of different parameters, the proposed method and other methods are compared.

1) COST AND EFFECT OF NOISE

Due to the high dependency on communication links, the cost, noise, and delay of suggested methods in [26], [27] are high.

TABLE 6. Comparative assessment of the proposed strategy with existing methods.

Comparison Criterion	[26]	[27]	[28]	[29]	Proposed method
Cost	High	High	Low	Low	Low
Effect of fault resistance	High	Not considered	Not considered	Not considered	No effect
Operation time	High-200 ms	High-120 ms	Low-13 ms	Low-30 ms	Low-84 ms
Effect of noise	High	High	Low	Low	Low
Application	PV relays	DC Temporary faults	DC Temporary faults	DC circuit breakers	DC Temporary faults
Maximum fault resistance (Ω)	2 Ω	0 Ω	0 Ω	0 Ω	3 Ω

However, the local DC coordination methods of [28], [29] and the proposed method have low cost and noise.

2) FAULT RESISTANCE

Considering the impact of fault resistance is one of the most important factors in coordinating different protection devices. In [27]–[29], the impact of fault resistance is not considered. Therefore, the outcomes of research cannot be implemented in practical situations. In [26] and proposed method, the impact of fault resistance is considered, and the maximum value of fault resistance in [26] and the proposed method are 2 Ω , and 3 Ω , respectively.

3) OPERATION TIME

Typically, coordination strategies using a time interval between protection devices, and appropriate coordination methods should consider this interval time and reduce the operation time of protection devices. The operation times of [26], [27] are 200 ms and 120 ms, respectively, which are high. And the operation times of [28], [29] and proposed scheme are 13 ms, 30 ms, and 84 ms, respectively, which are categorized into low operation times.

Consequently, the proposed method has low operation time, cost, and noise due to the lack of communication link, and proper coordination method between recloser switch and fuses. Therefore, these advantages make it more reasonable to implement the proposed scheme on the DC Microgrids.

V. CONCLUSION

A new recloser switch – fuse coordination strategy based on the time-current characteristic was proposed for DC microgrids in this paper. Despite the other methods which only can be used in AC systems, the proposed method was designed to implement in the DC microgrids. This approach uses the fault current magnitude and time to reach the maximum for the setting of the recloser switch. The new strategy uses only local measurements and does not require any communication links. Thus it increases the reliability and reduces the cost of the proposed scheme. The proposed strategy was validated by offline digital time-domain simulation studies in MATLAB/Simulink software environment for different fault types and resistances. Then, the results were compared with other reported strategies. Based on the obtained simulations and comparisons, it was found that the proposed method is

fast and inexpensive in different scenarios. Moreover, the new characteristic can be robust against the variations in the injected power of RERs and fault resistances and can save the fuses during the temporary faults.

REFERENCES

- [1] Y. Xu, H. Sun, and W. Gu, "A novel discounted min-consensus algorithm for optimal electrical power trading in grid-connected DC microgrids," *IEEE Trans. Ind. Electron.*, vol. 66, no. 11, pp. 8474–8484, Nov. 2019.
- [2] M. R. Habibi, H. R. Baghaee, T. Dragicevic, and F. Blaabjerg, "Detection of false data injection cyber-attacks in DC microgrids based on recurrent neural networks," *IEEE J. Emerg. Sel. Topics Power Electron.*, early access, Jan. 20, 2020, doi: [10.1109/JESTPE.2020.2968243](https://doi.org/10.1109/JESTPE.2020.2968243).
- [3] N. Bayati, A. Hajizadeh, and M. Soltani, "Protection in DC microgrids: A comparative review," *IET Smart Grid*, vol. 1, no. 3, pp. 66–75, Oct. 2018.
- [4] A. A. S. Emhemed, K. Fong, S. Fletcher, and G. M. Burt, "Validation of fast and selective protection scheme for an LVDC distribution network," *IEEE Trans. Power Del.*, vol. 32, no. 3, pp. 1432–1440, Jun. 2017.
- [5] S. Dhar, R. K. Patnaik, and P. K. Dash, "Fault detection and location of photovoltaic based DC microgrid using differential protection strategy," *IEEE Trans. Smart Grid*, vol. 9, no. 5, pp. 4303–4312, Sep. 2018.
- [6] S.-Y. Lee, Y.-K. Son, H.-J. Cho, S.-K. Sul, S.-H. Kim, N.-S. Kang, and W.-J. Park, "Simplified thermal model of semiconductor fuse for DC distribution system," in *Proc. 10th Int. Conf. Power Electron. ECCE Asia (ICPE-ECCE Asia)*, Busan, South Korea, May 2019, pp. 2641–2646.
- [7] M. N. Alam, B. Das, and V. Pant, "Optimum recloser–fuse coordination for radial distribution systems in the presence of multiple distributed generations," *IET Gener., Transmiss. Distrib.*, vol. 12, no. 11, pp. 2585–2594, Jun. 2018.
- [8] R. C. Dugan, M. F. McGranaghan, H. W. Beaty, *Electrical Power Systems Quality*. New York, NY, USA: McGraw-Hill, 2004.
- [9] T. A. Short, *Electric Power Distribution Handbook*. Boca Raton, FL, USA: CRC Press, 2004.
- [10] S. Santoso and T. A. Short, "Identification of fuse and recloser operations in a radial distribution system," *IEEE Trans. Power Del.*, vol. 22, no. 4, pp. 2370–2377, Oct. 2007.
- [11] S. M. Brahma and A. A. Girgis, "Development of adaptive protection scheme for distribution systems with high penetration of distributed generation," *IEEE Trans. Power Del.*, vol. 19, no. 1, pp. 56–63, Jan. 2004.
- [12] B. Hussain, S. M. Sharkh, S. Hussain, and M. A. Abusara, "An adaptive relaying scheme for fuse saving in distribution networks with distributed generation," *IEEE Trans. Power Del.*, vol. 28, no. 2, pp. 669–677, Apr. 2013.
- [13] S. Chaitusaney and A. Yokoyama, "Prevention of reliability degradation from Recloser–Fuse miscoordination due to distributed generation," *IEEE Trans. Power Del.*, vol. 23, no. 4, pp. 2545–2554, Oct. 2008.
- [14] A. F. Naiem, Y. Hegazy, A. Y. Abdelaziz, and M. A. Elsharkawy, "A classification technique for recloser–fuse coordination in distribution systems with distributed generation," *IEEE Trans. Power Del.*, vol. 27, no. 1, pp. 176–185, Jan. 2012.
- [15] H. Yazdanpanahi, Y. W. Li, and W. Xu, "A new control strategy to mitigate the impact of inverter-based DGs on protection system," *IEEE Trans. Smart Grid*, vol. 3, no. 3, pp. 1427–1436, Sep. 2012.
- [16] G. Stapleton and S. Neill, *Grid-Connected Solar Electric Systems the Earths can Expert Handbook for Planning, Design and Installation*. Evanston, IL, USA: Routledge, Nov. 2012.

- [17] J. vom Dorp, S. E. Berberich, A. J. Bauer, and H. Rysse, "Analysis of the DC-arc behavior of a novel 3D-active fuse," *Solid-State Electron.*, vol. 53, no. 7, pp. 809–813, Jul. 2009.
- [18] T. Tanaka, H. Kawaguchi, T. Terao, T. Babasaki, and M. Yamasaki, "Modeling of fuses for DC power supply systems including arcing time analysis," in *Proc. 29th Int. Telecommun. Energy Conf. (INTELEC)*, Rome, Italy, 2007, pp. 135–141.
- [19] S. Jamali, S. Bukhari, M. Khan, M. Mehdi, C. H. Noh, G. H. Gwon, and C. H. Kim, "Protection scheme of the last-mile active LVDC distribution network with reclosing option," *Energies*, vol. 11, no. 5, pp. 1093–1113, May 2018.
- [20] X. Pei, G. Tang, and S. Zhang, "Sequential auto-reclosing strategy for hybrid HVDC breakers in VSC-based DC grids," *J. Modern Power Syst. Clean Energy*, vol. 7, no. 3, pp. 633–643, May 2019.
- [21] J.-Y. Kim, S.-S. Choi, and I.-D. Kim, "A new reclosing and re-breaking DC thyristor circuit breaker for DC distribution applications," *J. Power Electron.*, vol. 17, no. 1, pp. 272–281, Jan. 2017.
- [22] M. Fang, L. Fu, R. Wang, and Z. Ye, "Coordination protection for DC distribution network in DC zonal shipboard power system," in *Proc. Int. Conf. Adv. Power Syst. Autom. Protection*, Beijing, China, Oct. 2011, pp. 418–421.
- [23] C. Cline and J. Stultz, "Fuse protection of DC systems," in *Proc. Amer. Power Conf.*, vol. 57. Chicago, IL, USA: Illinois Institute of Technology, Apr. 1995, p. 20.
- [24] N. Bayati, A. Dadkhah, S. H. H. Sadeghi, B. Vahidi, and A. E. Milani, "Considering variations of network topology in optimal relay coordination using time-current-voltage characteristic," in *Proc. IEEE Int. Conf. Environ. Electr. Eng. IEEE Ind. Commercial Power Syst. Eur. (EEEIC/I CPS Eur.)*, Milan, Italy, Jun. 2017, pp. 1–5.
- [25] S. D. A. Fletcher, P. J. Norman, K. Fong, S. J. Galloway, and G. M. Burt, "High-speed differential protection for smart DC distribution systems," *IEEE Trans. Smart Grid*, vol. 5, no. 5, pp. 2610–2617, Sep. 2014.
- [26] J. Naik, S. Dhar, and P. K. Dash, "Adaptive differential relay coordination for PV DC microgrid using a new kernel based time-frequency transform," *Int. J. Electr. Power Energy Syst.*, vol. 106, pp. 56–67, Mar. 2019.
- [27] Y. Xu, D. Shi, and S. Qiu, "Protection coordination of meshed MMC-MTDC transmission systems under DC faults," in *Proc. IEEE Int. Conf. IEEE Region 10 (TENCON)*, Xi'an, China, Oct. 2013, pp. 1–5.
- [28] X. Zheng, R. Jia, L. Gong, G. Zhang, and X. Pei, "An optimized coordination strategy between line main protection and hybrid DC breakers for VSC-based DC grids using overhead transmission lines," *Energies*, vol. 12, no. 8, p. 1462, Apr. 2019.
- [29] Y. Wang, Z. Yuan, J. Fu, Y. Li, and Y. Zhao, "A feasible coordination protection strategy for MMC-MTDC systems under DC faults," *Int. J. Electr. Power Energy Syst.*, vol. 90, pp. 103–111, Sep. 2017.



HAMID REZA BAGHAEI (Member, IEEE) was born in Kashan, Iran, in June 1984. He received the Ph.D. degree in electrical engineering from the Amirkabir University of Technology (AUT), in 2017.

From 2007 to 2017, he had been a Teaching and Research Assistant with the Department of Electrical Engineering, AUT. In August 2019, he joined AUT as an Associate Research Professor with the Department of Electrical Engineering. Since January 2020, he joined Shahid Beheshti University as a Guest Lecturer at the Department of Electrical Engineering. He is the author of one book, two published chapter books, 60 journal articles, and 55 conference papers, and owner of a registered patent. Up to now, among his journal articles, he has three HOT articles and seven HIGHLY-CITED articles, based on SciVal and Web of Science statistics. He is currently the Project Coordinator of the AUT Pilot Microgrid Project as one of the sub-projects of Iran Grand (National) Smart Grid Project. His special fields of interest are micro and smart grids, cyber-physical systems, application of power electronics in power systems, distributed generation, renewable energy resources, FACTS CUSTOM power devices, HVDC systems, power system operation, control, and application of artificial intelligence in power systems. He is a member of scientific program committee of several IEEE conferences. He is also the winner of four national and international prizes, as the Best Dissertation Award, from Iranian scientific organization of smart grids (ISOSG), in December 2017, Iranian Energy Association (IEA), in February 2018, AUT, in December 2018, and the IEEE Iran Section, in May 2019, for his Ph.D. dissertation. He was selected as the top 1% reviewer of engineering, in September 2018, and the top 1% reviewer of engineering and cross-field, in September 2019. He is also the reviewer of several IEEE and IET journals and a Guest Editor of several special issues in IEEE, IET, Elsevier, and MDPI.



AMIN HAJIZADEH (Senior Member, IEEE) received the B.S. degree from Ferdowsi University, Mashad, Iran, in 2002, and the M.S. and Ph.D. degrees (Hons.) from the K. N. Toosi University of Technology, Tehran, Iran, in 2005 and 2010, respectively, all in electrical engineering. He held a postdoctoral position with the Norwegian University of Science and Technology, Trondheim, Norway, from 2015 to 2016. Since 2016, he has been an Associate Professor with the Department

of Energy Technology, Aalborg University. His current research interests include control of distributed energy resources, design and control of power electronic converters for microgrid, and marine power systems. He is also the reviewer of several IEEE and IET journals, a Guest Editor and an Associate Editor of several special issues in IEEE, IET, and Elsevier, and a member of scientific program committees of several IEEE conferences.



MOHSEN SOLTANI (Senior Member, IEEE) received the M.Sc. degree in electrical engineering from the Sharif University of Technology, Tehran, Iran, in 2004, and the Ph.D. degree in electrical and electronic engineering from Aalborg University, Aalborg, Denmark, in 2008. He was a Visiting Researcher with the Eindhoven University of Technology, in 2007. He fulfilled a Postdoctoral and an Assistant Professor program with Aalborg University, from 2008 to 2012. In 2010, he was

a Visiting Scholar with Stanford University. Since 2012, he has been an Associate Professor with the Department of Energy Technology, Aalborg University. In 2015, he completed a research leadership training program with Harvard Business School. His research interests include modeling, control, optimization, estimation, fault detection, and their applications to electromechanical and energy conversion systems, power electronics, wind turbines, and wind farms.



NAVID BAYATI was born in Arak, Iran, in 1992. He received the B.Sc. degree in electrical engineering from Arak University, Arak, in 2014, and the M.Sc. degree in electrical engineering from the Amirkabir University of Technology, Tehran, in 2017. He is currently pursuing the Ph.D. degree in electrical engineering (power systems) with the Department of Energy Technology, Aalborg University Esbjerg, Denmark. Since 2019, he has been involved in research with Loughborough University, U.K. His research interests are power system protection, DC microgrid, and fault detection and location of renewable energy resource-based systems. He is also a reviewer of IEEE and IET journals. He was a recipient of Top 1% Reviewer in the world, in 2019.